A Response-Surface Methodology for Rotor Airfoil Design
with Multiple Design Constraints

Se Min Lee[1], Jeong Hwan Sa[2], Sang Eon Jeon[3], Chang-Joo Kim[4], Soo Hyung Park[5*] and Ki Hoon Chung[6]

[1-5] Department of Aerospace Information Engineering, Konkuk University, Seoul, South Korea

[6] Rotor Team, Korea Aerospace Research Institute, Daejeon, South Korea

[1] E-mail: semin@konkuk.ac.kr / [2] E-mail: sa_c@naver.com / [3] E-mail: eonman@korea.com

[4] E-mail: cjkim@konkuk.ac.kr/ [5*] E-mail: pish@konkuk.ac.kr, Corresponding Author

[6] E-mail: khchung@kari.re.kr

ABSTRACT

The design optimization of airfoils has been carried out to enhance aerodynamic performance of rotors using the Response Surface Method (RSM) and a Navier-Stokes equation solver. A multiple RSM has been developed for easy and simultaneous handling of various constraints, originated from the design requirement of airfoils for those applications to the rotorcraft. In addition to the description of aerodynamic shape for airfoils by using the Hicks-Henne functions, the mean camber line is parameterized to improve the design sensitivity to the aerodynamic pitching moment of airfoils. The aerodynamic performance is predicted using the KFLOW, a Navier-Stokes equation solver with shear stress transport turbulence modeling. Aerodynamic performance measures of designed airfoils are compared to those of initial airfoils to show the flexibility in handling constraints and the improvement of aerodynamic performance of airfoils with the proposed method.

1. Introduction

The airfoil design for its application to the rotor blade is not an easy task mainly due to complex aerodynamic environments around the rotor. To cope with large and unsteady variation in Mach number and the angle of attack along the span-wise location of the blade, more than three different airfoils are designed and distributed along the radial position of a blade with different design requirements for each airfoil [1]. An airfoil for inboard section should have high maximum lift coefficient to retard unfavourable stall effect at low Mach number. On the other hand, an airfoil for tip region should have high drag divergence Mach number [2]. Also, the airfoil thickness should be considered to improve the manufacturability of blades.

In this study five shape functions based on the Hicks-Henne functions to are adopted to describe the surface geometry of airfoil. In addition four shape functions are used in order to allow the camber change. An airfoil design tool is required to have high flexibility and accuracy in handling complex design requirements. For this purpose, a multiple Response Surface Method (RSM) is proposed in this study. The response surfaces are generated for each performance measure of the airfoil [3]. After conforming the required accuracy of each response surface, it is used for airfoil design optimization [4].

The random optimization method is adopted in this study to find the optimum design point. Two different cases of design parameterization with or without camber variation are applied and compared to show the effectiveness of the shape function which allows the camber variation.

2. Numerical Method

2.1 Airfoil Design Requirements

Airfoil aerodynamic design requirements for its rotorcraft application should reflect complex operating conditions of blades and are mainly determined from previous experience and knowhow. Main design goal of airfoils is to improve both the hover Figure of Merit, FM, and the equivalent lift-to-drag ratio, $(L/D)_e$, of the rotor at high forward speed when airfoils are distributed along radial position of the rotor blade. Airfoil aerodynamic design requirements can be defined by translating

the above mentioned aerodynamic performance measures of the rotor into the those for the individual airfoils such as lift (C_L), drag(C_D), and pitching moment coefficients (C_M) as a function of Mach number and angle of attack. To improve the hover FM airfoils should have high lift-to-drag ratio (L/D) [5, 6]. The enhancement of $(L/D)_e$ at high forward speed can be achieved by retarding the drag divergence Mach number (M_{DD}) especially at the advancing side of blade tip region and by delaying the airfoil stall at inboard section. Also the pitching moment should be as low as possible in order to minimize the strength requirements of mechanical control system including pitch link rods.

Table. 1 Airfoil Design Requirements and the Baseline Airfoils

AERODYNAMIC PERFORMANCE MEASUREMENTS & CONFIGURARIONS		SECTIONS		
		1	2	3
M_{DD} at $c_l = 0$	$\geq$	0.75	0.85	0.91
$\left| C_{m_n} \right|$ at $M = 0.7$	$\geq$	0.005	0.01	0.01
L/D at $M = 0.6$	$\geq$	free	64	76
C_{lmax} at $M = 0.4$	$\geq$	max	1.20	1.1
Max t/c, %		12	9	7
Baseline airfoil		OA 312	OA309	OA 407

This paper follows the airfoil design requirements similar to those defined through the Aerospatiale's experience [7] as shown in Table. 1. Three airfoils are assigned to inboard section (section 1), mid section (section 2), and tip section (section 3), respectively. The C_M is lower than 0.01 for all airfoils [7] and airfoils for the inboard portion of rotor are thicker than that of tip section to enhance stall character and improve manufacturability. The favourable range of M_{DD}, L/D, and maximum lift coefficient $(C_L)_{max}$ are allocated for each airfoil.

Numerical optimization problem for airfoil design requires careful selection for objective and constraint functions in order to meet all design requirements shown in Table 1. The airfoil for section 1 is designed by defining $(C_L)_{max}$ as the objective function. The previous design experiences show the simultaneous achievement of both $(C_L)_{max}$ and high M_{DD} is not easy. For the airfoil of Section 2, the drag coefficient is minimized with the fixed M_{DD} of 0.85. The design requirement for the C_M, L/D, and $(C_L)_{max}$ are treated as the constraints. The airfoil for tip section is designed by minimizing the C_D at Mach number of 0.91.

2.2 Airfoil Shape Functions and Design Variables

The Hicks-Henne functions are well known for its smooth surface generation of airfoils with relatively small number of parameters and widely used in various airfoil design studies. In this study five shape functions are adopted to generate upper and lower surfaces of each airfoil. In addition the mean chamber is expressed with four additional shape functions in order to enhance design sensitivity of chamber change to the C_M. Therefore, 14 design variables per airfoil are used in design optimization. The Hicks-Henne functions used for airfoil surface generation are expressed in Eqs (1)~(3) [8] and shape functions for the chamber distribution are defined as in Eqs (4)-(5).

$$f_1 = \frac{x^{1/2}(1-x)}{e^{15x}} \tag{1}$$

$$f_k = \sin(\pi x^{C_k})^3, k = 2,\cdots,5 \tag{2}$$

$$C_k = \frac{\log 0.5}{\log\left(\frac{k-1}{5}\right)} \tag{3}$$

$$g_n = -\sin\left(\pi(1-x)^{D_n}\right)^3, n = 1,2,3,4 \tag{4}$$

$$D_n = (\log 0.5)/\left(\log\frac{n}{5}\right) \tag{5}$$
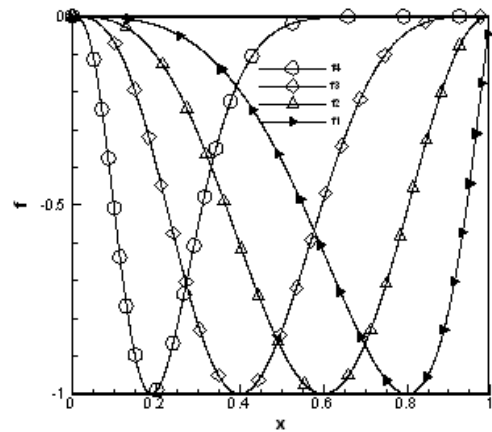

Fig. 1 Diagram of shape functions for mean camber line

Fig. 1 shows shape functions for camber distribution. The upper surface y_U and lower surface y_L of an airfoil can be parameterized as

$$y_L = y_{L0} + \sum_{i=1}^{5} d_{i,L} f_i + y_{C0} + \sum_{n=1}^{4} d_{n,C} g_n \tag{6}$$

$$y_U = y_{U0} + \sum_{i=1}^{5} d_{i,U} f_i + y_{C0} + \sum_{n=1}^{4} d_{n,C} g_n$$

where $y_{L0}, y_{C0}, y_{U0}, y_{C0}$ represent coordinates for upper and lower surfaces and camber distribution for the initial airfoil. Therefore, an airfoil can be design by determining the following design variables

$$\mathbf{d} = [d_{1,L}, \cdots, d_{5,L}, d_{1,U}, \cdots, d_{5,U}, d_{1,C}, \cdots, d_{4,C}]^T \quad (7)$$
$$= [d_1, d_2, d_3, \cdots, d_{14}]^T$$

2.3 Multiple Response Surface Method

The RSM is widely used in optimization problem with large number of design variables since the influence of each variable on the objective and constraint functions can be easily reflected without complex manipulation. The RSM approximates numerical or experimental database with minimum error in the least square sense [4]. Fig. 2 shows the design process using the multiple RSM. With an initial baseline airfoil, the design variables are all zeros ($\mathbf{d=0}$). In this study 200-points of design variable vector ($\mathbf{d}_k$, k=1,$\cdots$,**200**) are used to generate Response surfaces (RS). Each component d_j (j=1,$\cdots$,14) of design vector $\mathbf{d}_k$ (k=1,$\cdots$,200) is generated using the random number generator,. If the maximum thickness variation with a design variable vector $\mathbf{d}_k$ is greater than 10% of initial thickness, the corresponding vector $\mathbf{d}_k$ is discarded and regenerated.

After defining all required 200 points of design variable vectors, the flow solver, KFLOW, computes aerodynamic characteristics defined in Table. 1 for all airfoil configurations defined by $\mathbf{d}_k$, (k=1,$\cdots$,200) to build the aerodynamic database for the current design variable set $\mathbf{d}_k$.

The RSs for each of M_{DD}, $(C_L)_{max}$, L/D and C_{M0} are generated. In this study the quadratic function of the design variable vector is used to build each RS. To reserve the required accuracy of the response surface, the errors between data points in data base and the approximated values using the response surface are compared. Whenever the error of any RS is greater than the given tolerance, 10% among the design variable vectors are discarded and replaced with new vectors. This process is continued until all errors of each RS is less than the tolerance.

The airfoil design is started with the RS functions. There are 2 different approaches to design optimization. One is to use the general nonlinear programming (NLP) solver and the other is to use the random optimization method. This study uses the

later method to avoid the numerical difficulties with NLP solvers. For this purpose one design variable vector is generated using the random number generator. In case this vector violates one of design constraints or it generates poor airfoil performance than that with the previous best selection of the design variable vector. This process is continued until the improvement in objective function value is less that the given tolerance. This process guarantees the automatic satisfaction of all design constraints.
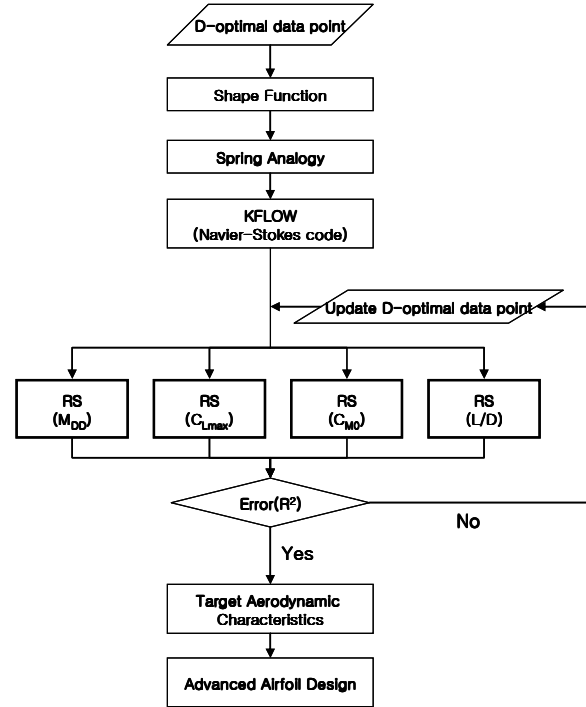

Fig. 2 Diagram of design process

2.4 Flow Solver

The aerodynamic coefficients of airfoils are predicted using the KFLOW which resolve the 2-D compressible Navier-Stokes equations with the $k-\omega$ Shear Stress Transport (SST) turbulence model. The viscosity coefficient predicted using the SST turbulent model can consider the major transfer characteristics of turbulence shear stress, related to flows with adverse pressure gradient. The Roe's FDS (Flux Difference Splitting) and 2nd order unwind MUSCL schemes are used for spatial discretization and the diagonalized ADI scheme is applied to get an accelerated steady-state solution [9].

The C-type computational grid with the 321x65 points is generated and modified whenever a new airfoil shape is defined. In this research the spring analogy concept is applied to regenerate computational grid during shape design process

[10]. This approach provides an efficient generation of new grid with equal level of smoothness and orthogonality as those of the original grid system.

3. Applications to Airfoil Design

In this study two different cases of design parameterization are applied and compared the design results of each airfoil for section 1~ section 3. Two cases are classified depending on whether the shape function for camber is included or not. In case the shape function for camber is not included, the results in figures are marked with P.M. which represents the general method of previous researchers.

3.1 Airfoil Design for Section 1

Fig.3 shows the comparison of the shape of the baseline airfoil and those of the designed airfoils. KU 112 represents the design result with camber change. The results, KU 112-P.M. , without camber change has nearly the same chamber distribution as that of the baseline airfoil, which denotes the Hicks-Henne functions defined in Eqs (1)~(3) hardly change camber distribution. Fig.4 compares the lift coefficients. The designed airfoils has $(C_L)_{max}$ greater than that of design requirements of $(C_L)_{max}$ =1.7. The lift curve slope is nearly the same as that of the baseline airfoil. In this design case, the design requirement for L/D is not applied since this constraint can restrict the increase in $(C_L)_{max}$.

Fig. 5 depicts the ratio L/D of the airfoil sections plotted against the angle of attack. The maximum L/D is achieved around the angle of attack of 3 degrees. The result of KU 112 is similar to the baseline airfoil while KU 112_P.M. shows the ratio L/D decrease as the angle of attack is further increased. This result represents difficulty in simultaneous improvement of both the ratio L/D and $(C_L)_{max}$. Fig. 6 shows the variation of drag and moment coefficients with varying Mach number. KU 112 airfoil has the lower C_D and the higher M_{DD} (defined as $\partial C_d / \partial M = 0.1$) compared to those of the baseline and KU 112_P.M. airfoil. Furthermore KU 112 airfoil has better moment characteristic than that of the baseline airfoil. All of the designed airfoils satisfy the design requirements for M_{DD} and C_M.

The designed airfoil with camber change shows better performance compared to that without camber change in that it shows higher M_{DD} and lower C_M.

3.2 Design optimization of Section 2

Fig. 7 shows the airfoil shape change after design optimization. The plot for KU 109 airfoil represents the camber variation from that of the baseline airfoil.

Fig. 8 compares the lift coefficients. The designed airfoils has greater $(C_L)_{max}$ satisfying the design constraints of $(C_L)_{max}$ =1.2. The lift curve slope is nearly the same as that of the baseline airfoil. Fig. 9 shows the ratio L/D of the airfoil sections plotted against the angle of attack. The maximum L/D is achieved around the angle of attack of 4 degrees.

Fig. 10 represents the variation of drag and moment coefficients with varying Mach number. The C_D of KU 109 airfoil show gradual increase at Mach number of 0.8, while the C_D of KU 109_P.M. airfoil has increased rapidly. The C_M of KU 109 airfoil is close to zero over the Mach number range to M_{DD}. All of the designed airfoils satisfy the design requirements of $M_{DD} > 0.85$ and $|C_M| < 0.01$.

3.3 Design optimization of Section 3

Fig. 11 shows the comparison of the shape of the baseline airfoil and those of the designed airfoils. KU 107 and KU 107_P.M. airfoils show significant change in the surfaces compared to the baseline airfoil,.

The objective function is minimum the C_D at Mach number of 0.91. Both KU 107 and KU 107_P.M. airfoils violates M_{DD} constraint as shown in Fig. 14. Mach number of 0.91 is quite challenging value compared to that of the baseline airfoil. The C_M of designed airfoils fully satisfies the design requirement, but improvements are much lower than the results of Section 3.2.

4. Conclusion

The design optimization of airfoil for the application has been carried out for its applications to rotorcraft using multiple RSM and the flow solver of Navier-Stokes equation. The shape functions which allow camber change are proposed to enhance design sensitivity of camber. By adding these functions, the airfoils with better performance can be designed. The results of this study show a multiple response surface method can be effectively applicable for the aerodynamic design of airfoils.
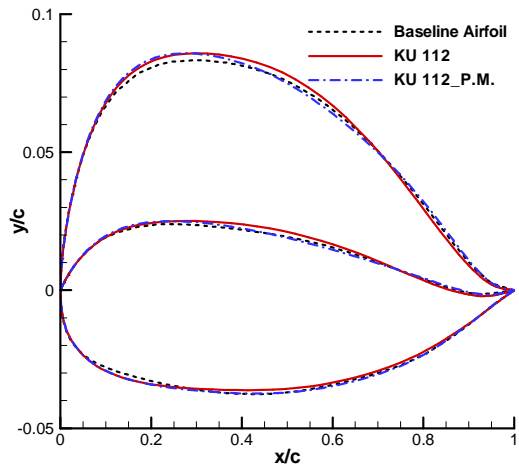
Fig. 3 Comparison of the Baseline Airfoil and Designed Airfoils
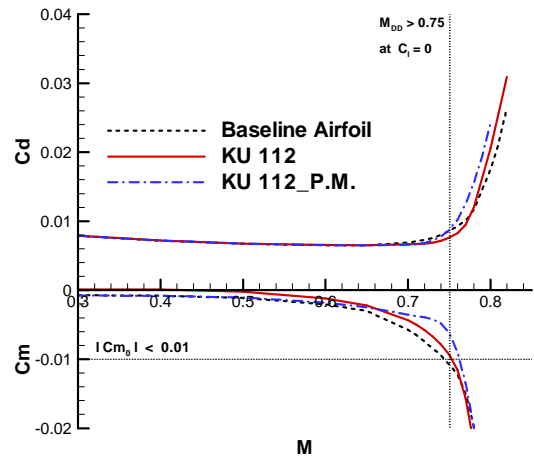

Fig. 6 Computed drag and moment characteristics of the Baseline Airfoil and Designed Airfoils, $Re = M \times 8 \times 10^6$.
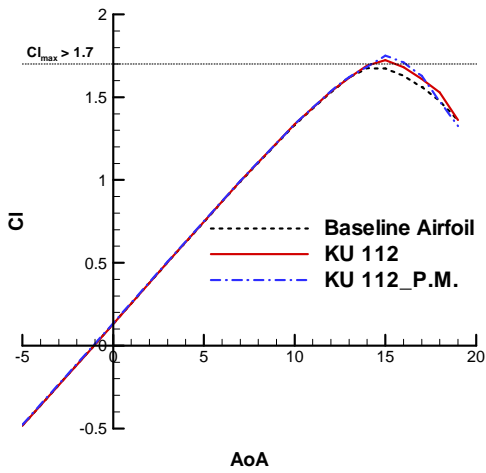

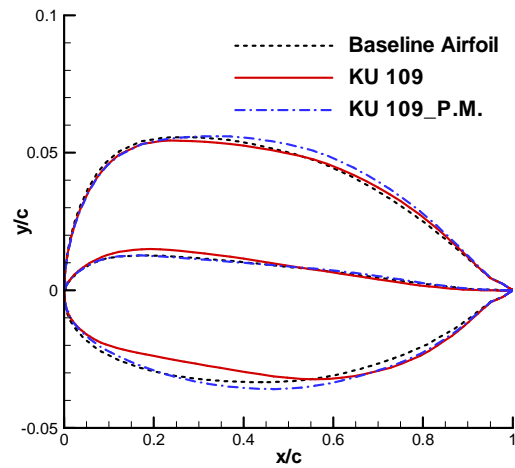Fig. 4 Lift curve slope of the Baseline Airfoil and Designed Airfoils, $M = 0.4, Re = 3.2 \times 10^6$.

Fig. 7 Comparison of the Baseline Airfoil and Designed Airfoils
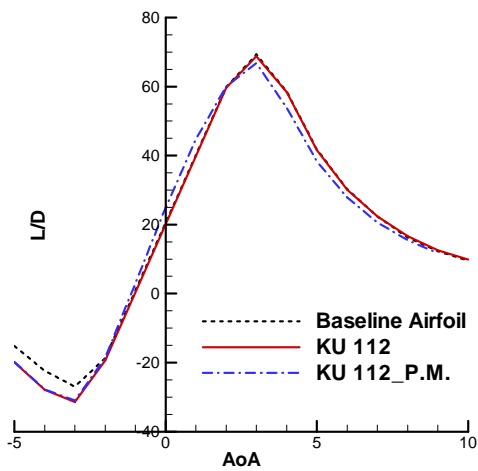

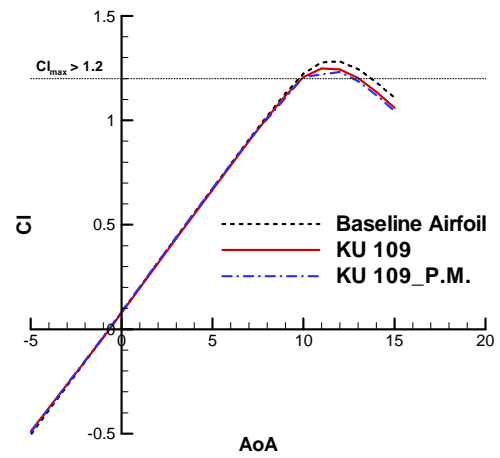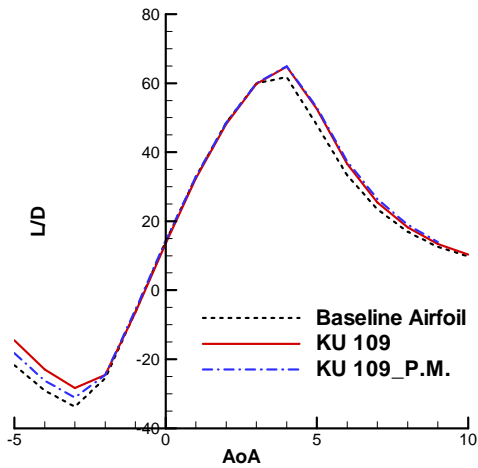Fig. 5 Lift to drag ratio of the Baseline Airfoil and Designed Airfoils, $M = 0.6, Re = 4.8 \times 10^6$.

Fig. 8 Lift curve slope of the Baseline Airfoil and Designed Airfoils, $M = 0.4, Re = 3.2 \times 10^6$.

Fig. 9 Lift to drag ratio of the Baseline Airfoil and Designed Airfoils, $M = 0.6$, $Re = 4.8 \times 10^6$.
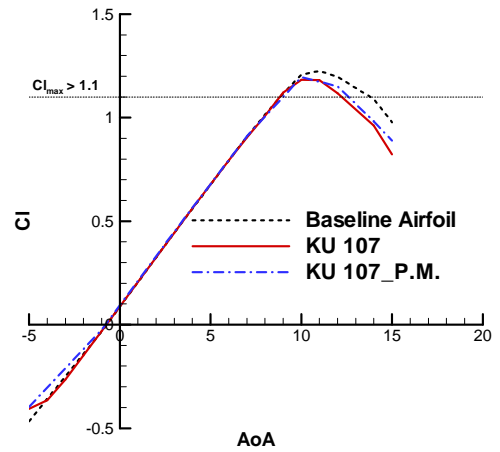

Fig. 12 Lift curve slope of the Baseline Airfoil and Designed Airfoils, $M = 0.4$, $Re = 3.2 \times 10^6$.
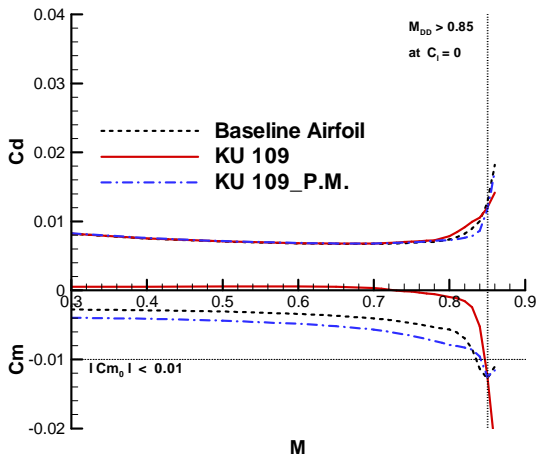

Fig. 10 Computed drag and moment characteristics of the Baseline Airfoil and Designed Airfoils, $Re = M \times 8 \times 10^6$.
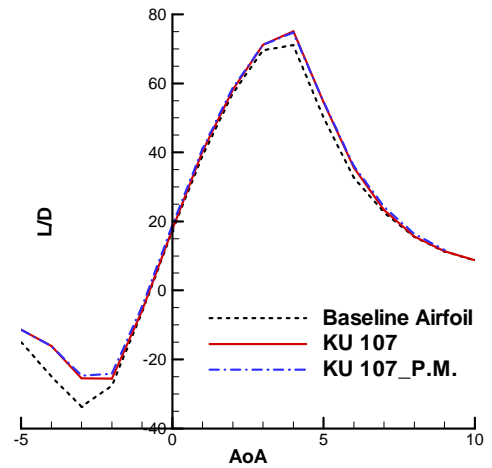

Fig. 13 Lift to drag ratio of the Baseline Airfoil and Designed Airfoils, $M = 0.6$, $Re = 4.8 \times 10^6$.
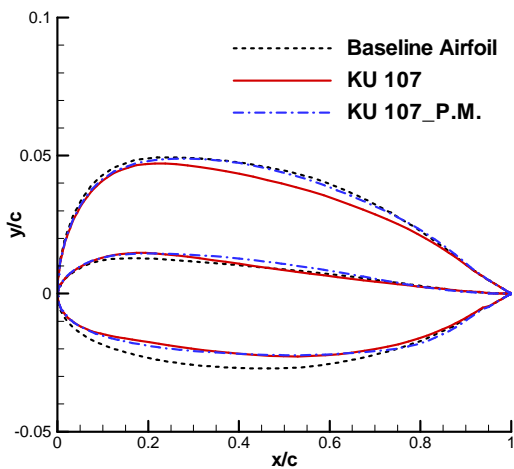

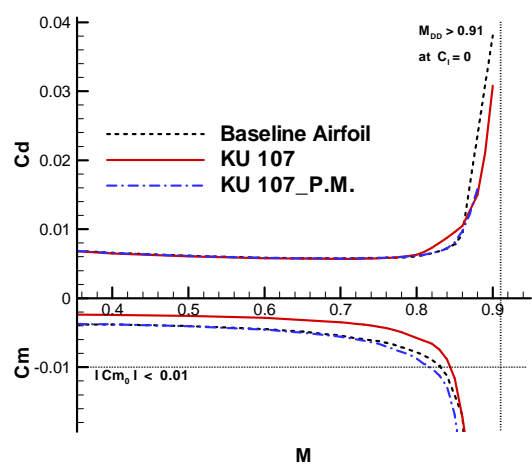Fig. 11 Comparison of the Baseline Airfoil and Designed Airfoils

Fig. 14 Computed drag and moment characteristics of the Baseline Airfoil and Designed Airfoils, $Re = M \times 8 \times 10^6$.

Acknowledgement

References

[1] Jones, B.R., Crossley, W.A., and Lyrintzis, A.S., "Aerodynamic and Aeroacoustic Optimization of Rotorcraft Airfoils via a Parallel Genetic Algorithm," *Journal of Aircraft*, Vol.37, No.6, pp.1088-1096, 2000.

[2] Dadone, L.U., "Design and Analytical Study of a Rotor Airfoil," NASA Contractor Report, NASA CR-2988, 1978.

[3] Sa, J.H., Park, S.H., Kim, C-J., Yun, C.Y., Kim, S.H., Kim, S.H., and Yu, Y.H., "Aerodynamic Design Optimization of Rotor Blade OA Airfoils" *KSCFE*, Vol.14, No.2, pp.25-31, 2009.

[4] Myers, R.H., and Montgomery, D.C., Response Surface Methodology, John Wiley and Sons, New York, NY, USA, 2002.

[5] Bousman, W.G., "Airfoil Design and Rotorcraft Performance," 58th AHS Forum, Montreal, Canada, 2002.

[6] Wortmann, F.X., and Drees, J.M., "Design of Airfoils for Rotors," CAL/AVLABS 1969 Symposium on Aerodynamics of Rotary Wing and VTOL Aircraft, 1969.

[7] Vuillet, A., "Rotor and Blade Aerodynamic Design," AGARD-FDP Special course on Aerodynamics of Rotorcraft, VKI, Brussels, Belgium, 1990.

[8] Hicks, R.M., and Henne, P.A., "Wing design by numerical optimization," *Journal of Aircraft*, Vol.15, No7, pp.407-412, 1978.

[9] Park, S.H., and Kwon, J.H., "Implementation of $k-\omega$ Turbulence Models in an Implicit Multigrid Method," *AIAA journal*, Vol.42, No.7, pp.1348-1357, 2004.

[10] Batina, J.T., Robinson, B.A., and Yang, H.T., "Aeroelastic analysis of wings using the Euler equations with a deforming mesh," NASA Technical Memorandum, NASA TM-102733, 1990.